ACS APPLIED MATERIALS & INTERFACES

Letter

www.acsami.org

Structural and Thermal Disorder of Solution-Processed $CH_3NH_3PbBr_3$ Hybrid Perovskite Thin Films

Christoph Wolf,[†] Joo-Sung Kim,[†,‡] and Tae-Woo Lee*[,‡]

[†]Department of Materials Science and Engineering, Pohang University of Science and Technology (POSTECH). Pohang, Gyungbuk 37673, Republic of Korea

[‡]Department of Materials Science and Engineering, Seoul National University, 1 Gwanak-ro, Gwanak-gu, Seoul 08826, Republic of Korea

Supporting Information

ABSTRACT: We extracted the electronic disorder energy of the organic−inorganic lead-halide hybrid perovskite $CH_3NH_3PbBr_3$ from temperature-dependent absorption data. We showed that the disorder at room temperature is ∼30 meV and is due to strong electron−phonon coupling with the longitudinal-optical mode of energy 16 meV. This mode can be attributed to longitudinal-optical phonons of the inorganic $PbBr_6$ frame; this conclusion highlights the polaronic nature of electronic excitations in $CH_3NH_3PbBr_3$. We showed that structural disorder is of the same impact as thermal disorder. A temperature-dependence of the exciton binding energy was observed close to the orthorhombic-to-tetragonal phase-transition temperature.

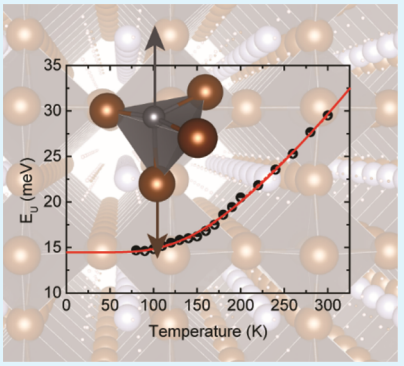

KEYWORDS: *hybrid lead-halide perovskite, disorder, Urbach energy, spectroscopy, exciton binding energy*

$CH_3NH_3PbX_3$ (CH_3NH_3 = methylammonium MA, X = Cl, Br, I) organic−inorganic perovskites (OIP) are solution-processable semiconductors, compatible with low-cost, low-temperature fabrication. The thermodynamic stability of OIP decreases in the sequence Cl > Br > I; $MAPbI_3$ is thermodynamically unstable and degrades to PbI_2 and MAI over time.[1] The band gap follows the same order Cl > Br> I, so $MAPbCl_3$ is not attractive as light absorber in solar cells. Because of these trends, $MAPbBr_3$ is an excellent compromise between thermodynamic stability and band gap (2.3 eV); as a result, solar cells that use $MAPbBr_3$ have high open-circuit voltage and decent power-conversion efficiency, and can be expected to exhibit long-time structural stability of the absorber material.[2]

The fabrication of flat, pinhole free $MAPbBr_3$ films has proven difficult. A variety of methods have surfaced that produce dense films and tailor the film properties to a particular application. For example, increase in grain size can increase the energy conversion efficiency in solar cells,[3] but can decrease the luminous efficiency of light-emitting diodes.[4] Which traits characterize "good" or "bad" active layers are not clear. Studies have correlated device performance with grain size,[3,4] film roughness,[5] and electronic disorder,[6,7] among other parameters. Remarkably, the electronic disorder obtainable from solution-processing has been found to be low, rivaling inorganic semiconductor that usually require high vacuum processing from high purity materials (see Table S1).

Here, we investigate the origin of electronic disorder in polycrystalline $MAPbBr_3$ thin films fabricated by direct, single-step solution process. Temperature-dependent absorption spectroscopy was used to distinguish structural (chemical) from thermal disorder. Both types of disorder were low, so the absolute magnitude of Urbach energy E_u was ∼30 meV at room temperature (RT) with the dominating coupling being to the lead-halide vibration mode of 16 meV. We report the temperature-dependence of the exciton binding energy that changes at the phase transition temperature T_{PT} = 150 K, which is in good agreement with previous reports on the discontinuity of the dielectric constant.[8]

Thin films of $MAPbBr_3$ were fabricated by mixing equimolar portions of MABr and $PbBr_2$ to form a 40 wt % solution in DMSO. The solution was spin-coated on cleaned glass in a glovebox under N_2 atmosphere. Fast crystallization was initiated by dripping chloroform during the spin-coating process, resulting in flat, low surface-roughness, 400 nm thick films free of pin-holes. Films were thermally annealed at 90 °C for 10 min resulting in a polycrystalline film with surface roughness R_q < 30 nm and grain sizes following a normal distribution with $\mu + \sigma$ of 400 + 170 nm (more details on the film fabrication and characterization are presented in the Note S1 and Figures S1−S4). Temperature was controlled using an

Received: December 7, 2016
Accepted: March 14, 2017
Published: March 14, 2017

DOI: 10.1021/acsami.6b15694
ACS Appl. Mater. Interfaces 2017, 9, 10344−10348

Oxford instrument liquid nitrogen cryostat with the sample in exchange gas (Oxford DN-2), and a custom-written temperature-control program that equilibrated the temperature for 1 min after reaching the set temperature before the data were collected. Absorption data were measured by a SCINCO S-3100 multichannel spectrophotometer. For photoluminescence measurements, a 405 nm pulsed (80 MHz, $P \leq 0.4$ mW) laser-diode (PicoQuant GmbH, LDH-405) was used as excitation source and the emission spectra were collected using a StellarNet inc. BlueWave fiber coupled spectrometer.

Temperature-dependent absorption data are presented in Figure 1a. A constant baseline was subtracted from the raw-

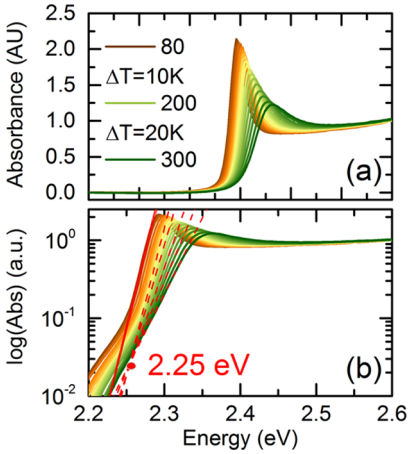

Figure 1. (a) Temperature-dependent absorption of $MAPbBr_3$ at $80 \leq T \leq 300$ K. A constant baseline was removed from the raw data. (b) the same data presented on a log-scale used for calculation of the disorder energy. The intersection of fits for the temperature region above 150 K (dashed lines) is marked.

data. On a logarithmic scale (Figure 1b) all linear trends of absorption collected at $T > 150$ K intersected at $E_0 = 2.25$ eV, corresponding to the lowest band gap theoretically achievable in this material and phase and called Urbach focus. This value agrees well with literature values,[9] and our own diffuse reflectance measurements on single crystals of $MAPbBr_3$ (see Figure S5). Data collected at $T < 150$ K show nearly parallel lines; this is characteristic of structurally disordered materials.[10] For the low-temperature phase, the intersection lies close to $E_0 \approx 2.0$ eV.

The absorption data were used to calculate electronic disorder effects in semiconductor materials. Electronic disorder manifests itself in an exponential rise of the absorption edge in the form[11]

$$\alpha(E, T) = \alpha_0 \exp\left(\sigma(T)\frac{E - E_0}{k_B T}\right) \quad (1)$$

where α is the absorption coefficient as a function of energy E and absolute temperature T. α_0, E_0 ,and $\sigma(T)$ are treated as fitting parameters. $\sigma(T)$, usually roughly of order unity, is often referred to as the steepness parameter and $k_B = 8.617 \times 10^{-5}$ eV K^{-1} is the Boltzmann constant. The Urbach energy is defined as $E_u = k_B T \sigma (T)^{-1}$. Compared with eq 1, E_u is simply the inverse slope of ln $(\alpha(E, T))$ below the excitonic peak. Further, $\sigma(T)$ is related to the average phonon energy $\hbar\omega$ in the model by Redfield and Dow as[10,12]

$$\sigma(T) = \sigma_0\left(\frac{2k_B T}{\hbar\omega}\right)\tanh\left(\frac{\hbar\omega}{2k_B T}\right) \quad (2)$$

If σ follows eq 2, calculation of E_u is physically meaningful.

We find that E_u can further be partitioned into a structural (or intrinsic) E_1 (x) and thermal E_2 (T) term by adopting the model of an Einstein oscillator:[13]

$$E_u(x, T) = E_1(x) + \frac{E_2}{\exp\left(\frac{\Theta}{T}\right) - 1} \quad (3)$$

where Θ is the characteristic temperature of an Einstein solid, and is related to a Debye temperature by $\Theta_D = 4\Theta/3$.

$MAPbBr_3$ undergoes a phase transition from orthorhombic to tetragonal at 144.5 K, between tetragonal phases at 149.5 and 155 K, then to a cubic phase at >236.9 K.[14] The phase transitions are first-order, accompanied by large entropy (order−disorder type), and the low-temperature orthorhombic-to-tetragonal transition (at 144.5 K) is accompanied by a discontinuity in the dielectric constant.[8] No discontinuity was reported for the higher-temperature phase-transitions. The tetragonal-cubic transition is accompanied by a continuous change of lattice parameter.[15] The phase transition leads to a significant change in steepness parameter $\sigma(T)$ (Figure 2a)

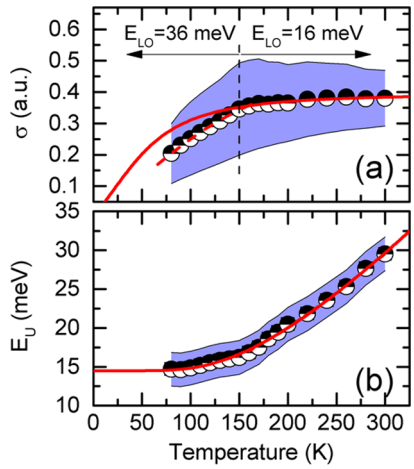

Figure 2. (a) Steepness parameter σ as a function of T. The solid line is the result of fitting eq 2 at $T > 150$ K and the dashed line is the same fit at temperatures below 150 K.E_{LO} shows a discontinuity at the phase transition temperature. (b) Disorder energy E_U as a function of T. The solid line corresponds to a fit of eq 3 to at $T > 150$. The shaded area represents the uncertainty (details given in Note S2).

accompanied by an increased phonon energy in the low-temperature phase, whereas the overall disorder (Figure 2b) is less affected because of the additivity of thermal and structural disorder.

Generally, the trends in the data at $150 \leq T \leq 300$ K, and the limited number of data points mean that our results can only be explained after careful comparison with the literature. The coupling between charge-carriers and a longitudinal optical (LO)-phonons with energy of 15.3 meV was reported previously,[16] which matches well with our lead-halide vibration mode of ∼16 meV. The origin of the increased value of phonon energy in the orthorhombic phase can be understood as follows; its energy matches the organic MA cation, but not the inorganic cage.[17] However, the MA cation is not directly involved in electronic processes, because the band extrema are

DOI: 10.1021/acsami.6b15694
ACS Appl. Mater. Interfaces 2017, 9, 10344−10348

formed by Pb and Br orbitals.[18] It has been suggested that a coupling mechanism between MA and the inorganic cage exists.[19] Neutron diffraction has revealed that in the low-temperature phase (<150 K) the MA hydrogen forms hydrogen bonds with Br.[20] A detailed study of the MA-dynamics in $MAPbBr_3$ by neutron inelastic scattering has confirmed that up to 150 K energy is transferred between organic and inorganic sublattice,[21] which agrees well with the temperature dependence of $\sigma(T)$ observed here. This finding is further supported by the lack of such a discontinuity in the related perovskite structure $CsPbBr_3$, where the organic MA cation has been replaced by the isotropic, inorganic cesium (Figure S6).

A generally similar behavior has been reported for the related material $MAPbI_3$,[22] in which the intrinsic disorder is of the magnitude of 20−30 meV with Θ = 200−350 K, which agrees well with our data. The results of the disorder analysis (eq 2, 3) below T = 150 K and above T = 150 K are summarized in Table I.

Table I. Results of Analysis of Disorder Energy for Phases of $MAPbBr_3$ at <150 K (orthorhombic) and above >150 K (tetragonal and cubic)[a]

phase	E_1 (meV)	E_2 (meV)	Θ (K)	σ_0(a.u.)	$\hbar\omega$ (meV)
<150 K	14 ± 1	10 ± 1	280 ± 100	0.54 ± 0.01	36 ± 1
>150 K	12 ± 4	36 ± 3	335 ± 60	0.40 ± 0.01	16 ± 2

[a]Error noted is the uncertainty of the fit alone and a lower bound. E_1, structural disorder; E_2, thermal contribution to the disorder; Θ, characteristic temperature; σ_0, steepness parameter; $\hbar\omega$, phonon energy.

Absorption data can be further analyzed. We extract band gap energy E_g and exciton binding energy E_b by deconvolution of the absorption data in exciton and band (continuum) contributions, in the framework of Elliott's absorption theory for excitons,[23] which we implement as recently applied to $MAPbBr_3$.[24] According to reports, the exciton binding energy in $MAPbBr_3$ lies between 40 and 60 meV when studied by optical spectroscopy (see also Table S2).[24−26] Interestingly, no temperature-dependence of E_b has been previously reported, although it had been suggested by calculation,[27] and the dielectric constant is discontinuous at the lowest phase-transition temperature.[8] Considering that E_b of an electron−hole pair (in effective-mass theory) is inversely proportional to the dielectric constant ε and directly proportional to the effective mass μ, a dependence $E_b \propto \mu/\varepsilon^2$ can be expected. Results of our data analysis are given in Figure 3a. In our measurement, E_b near the phase transition closely follows the reported trend of the dielectric function.[8,14] Above 150 K, the binding energy increases in a way not described by the dielectric function alone. With the large difference between static and high-frequency dielectric constant the strong polarizability of the lattice and associated polaron effects play most likely a role.[28] We estimate the uncertainty ΔE_b = 1 meV based on the spread of values in a series of measurements (details in Note S2).

We analyze the Stokes shift of our samples. OIP generally show a small shift between PL emission and absorption peak. Figure 3b shows absorption band gap and PL peak-center energy. The total shift at RT is ∼100 meV and the PL gradually shifts away from the from the band gap, an effect previously associated with phonon effects,[29] which is further exhibited in

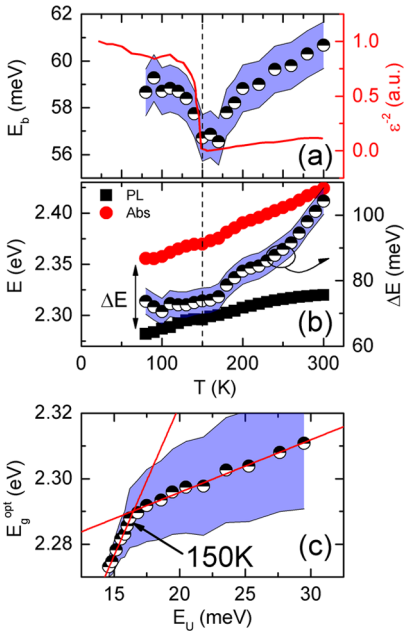

Figure 3. (a) Exciton binding energy E_b as a function of temperature as extracted from the excitonic part and the inverse square ε^{-2} of the dielectric constant.[8] The discontinuity of ε^{-2} agrees well with a change in exciton binding energy at the phase transition temperature. The total range of E_b is small. (b) Plot of exciton peak position from PL and band gap as a function of temperature T. The half-filled circles show the difference of band gap E_g and PL peak center energy: $\Delta E = E_g - E_{PL}$. (c) The Tauc band gap E_g^{opt} as a function of the calculated Urbach energy resulting in two regions of linear dependence that intersect at the phase-transition temperature 150 K.

continuous broadening of the PL peak with a characteristic energy of 16 meV (Figure S9). Thermal quenching of PL intensity (Figure S9) further supports the magnitude of our E_b = 60 meV.

Finally, we elucidate if structural and thermal disorder are of equal influence on the charge carrier. This manifests itself in a linear relationship between optical gap and disorder energy.[30] We calculate the optical band gap E_g^{opt} by Tauc's method assuming allowed direct transitions. Two regions exist, separated by the phase-transition temperature (Figure 3c), where E_g^{opt} and E_u have a linear relationship. Similar linear relationships are found between the PL peak width, band gap E_g and E_u (Figure S10). This indicates structural and thermal disorder have equivalent influence on the electronic state.

In conclusion, we have shown that deposition of $MAPbBr_3$ from a single-source precursor at RT leads to low structural disorder and moderate thermal disorder, typical for $MAPbX_3$ (X = halide) hybrid perovskites. The major source of thermal disorder is the coupling with an LO-phonon mode of energy E_{LO} = 16 ± 2 meV. The characteristic temperature of Θ = 335 ± 60 K indicates that all phonon modes should be excited at moderate temperatures. Relations between optical band gap and E_u are linear both below and above 150 K; this result indicates that structural and thermal disorder contribute equally to the total Urbach disorder. E_b extracted from the exciton line-shape is ∼60 meV and shows a discontinuity at 150 K, which is the temperature at which $MAPbBr_3$ changes from orthorhombic to tetragonal phase; this observation is consistent with the discontinuity in the dielectric constant at that transition.

DOI: 10.1021/acsami.6b15694
ACS Appl. Mater. Interfaces 2017, 9, 10344−10348

We expect that the insight into the nature of electronic disorder will guide further optimization of devices that use $MAPbBr_3$. Structural disorder obtainable from solution-processed polycrystalline thin films is low and thermal effects dominate the disorder at room temperature. We suggest that further improvement of device performance can be achieved by focusing on interfacial properties.

■ ASSOCIATED CONTENT

Supporting Information

The Supporting Information is available free of charge on the ACS Publications website at DOI: 10.1021/acsami.6b15694.

Details on the fabrication process of pinhole free $MAPbBr_3$ thin films and their characterization; diffuse reflectance measurement of single crystals and thin films; analysis of absorption data of $CsPbBr_3$ thin films, uncertainty and reproducibility analysis; supporting PL data (PDF)

■ AUTHOR INFORMATION

Corresponding Author

*E-mail: twlees@snu.ac.kr.

ORCID

Christoph Wolf: 0000-0002-9340-9782

Tae-Woo Lee: 0000-0002-6449-6725

Author Contributions

C.W. and J.-S.K. performed the experiments and wrote the manuscript. T.-W.L. improved the final manuscript. All authors have given approval to the final version of the manuscript.

Funding

This work was supported by the National Research Foundation of Korea (NRF) grant funded by the Korea government (Ministry of Science, ICT & Future Planning) (NRF-2016R1A3B1908431).

Notes

The authors declare no competing financial interest.

■ ACKNOWLEDGMENTS

C.W. is indebted to Professor Laura Herz of University of Oxford for stimulating discussions and to Ms. Lee Ho-Jeong for the diffuse reflectance measurements.

■ REFERENCES

(1) Nagabhushana, G. P.; Shivaramaiah, R.; Navrotsky, A. Direct Calorimetric Verification of Thermodynamic Instability of Lead Halide Hybrid Perovskites. *Proc. Natl. Acad. Sci. U. S. A.* **2016**, *113* (28), 7717−7721.

(2) Kulbak, M.; Cahen, D.; Hodes, G. How Important Is the Organic Part of Lead Halide Perovskite Photovoltaic Cells? Efficient CsPbBr3 Cells. *J. Phys. Chem. Lett.* **2015**, *6* (13), 2452−2456.

(3) Chen, Q.; Zhou, H.; Hong, Z.; Luo, S.; Duan, H. S.; Wang, H. H.; Liu, Y.; Li, G.; Yang, Y. Planar Heterojunction Perovskite Solar Cells via Vapor-Assisted Solution Process. *J. Am. Chem. Soc.* **2014**, *136* (2), 622−625.

(4) Cho, H.; Jeong, S.-H.; Park, M.-H.; Kim, Y.-H.; Wolf, C.; Lee, C.-L.; Heo, J. H.; Sadhanala, A.; Myoung, N.; Yoo, S.; Im, S. H.; Friend, R. H.; Lee, T.-W. Overcoming the Electroluminescence Efficiency Limitations of Perovskite Light-Emitting Diodes. *Science* **2015**, *350* (6265), 1222−1225.

(5) Longo, G.; Gil-Escrig, L.; Degen, M. J.; Sessolo, M.; Bolink, H. J. Perovskite Solar Cells Prepared by Flash Evaporation. *Chem. Commun.* **2015**, *51* (34), 7376−7378.

(6) Sadhanala, A.; Deschler, F.; Thomas, T. H.; Dutton, S. E.; Goedel, K. C.; Hanusch, F. C.; Lai, M. L.; Steiner, U.; Bein, T.; Docampo, P.; Cahen, D.; Friend, R. H. Preparation of Single Phase Films of CH 3 NH 3 Pb(I 1-X Br X) 3 with Sharp Optical Band Edges. *J. Phys. Chem. Lett.* **2014**, *5* (15), 2501−2505.

(7) De Wolf, S.; Holovsky, J.; Moon, S. J.; Löper, P.; Niesen, B.; Ledinsky, M.; Haug, F. J.; Yum, J. H.; Ballif, C. Organometallic Halide Perovskites: Sharp Optical Absorption Edge and Its Relation to Photovoltaic Performance. *J. Phys. Chem. Lett.* **2014**, *5* (6), 1035−1039.

(8) Onoda-Yamamuro, N.; Matsuo, T.; Suga, H. Dielectric Study of CH3NH3PbX3 (X = Cl, Br, I). *J. Phys. Chem. Solids* **1992**, *53* (7), 935−939.

(9) Leguy, A.; Azarhoosh, P.; Alonso, M. I.; Campoy-Quiles, M.; Weber, O. J.; Yao, J.; Bryant, D.; Weller, M. T.; Nelson, J.; Walsh, A.; van Schilfgaarde, M.; Barnes, P. R. F. Experimental and Theoretical Optical Properties of Methylammonium Lead Halide Perovskites. *Nanoscale* **2016**, *8*, 6317−6327.

(10) Studenyak, I.; Kranj, M.; Kurik, M. Urbach Rule in Solid State Physics. *Int. J. Opt. Appl.* **2014**, *4* (3), 76−83.

(11) Urbach, F. The Long-Wavelength Edge of Photographic Sensitivity and of the Electronic Absorption of Solids. *Phys. Rev.* **1953**, *92* (5), 1324.

(12) Dow, J. D.; Redfield, D. Toward a Unified Theory of Urbach's Rule and Exponential Absorption Edges. *Phys. Rev. B* **1972**, *5* (2), 594−610.

(13) Levcenko, S.; Syrbu, N. N.; Arushanov, E.; Tezlevan, V.; Fernández-Ruiz, R.; Merino, J. M.; León, M. Optical Properties of Monocrystalline CuIn5Se8. *J. Appl. Phys.* **2006**, *99* (7), 073513.

(14) Poglitsch, A.; Weber, D. Dynamic Disorder in Methylammoniumtrihalogenoplumbates (II) Observed by Millimeter-Wave Spectroscopy. *J. Chem. Phys.* **1987**, *87* (11), 6373.

(15) Kawamura, Y.; Mashiyama, H.; Hasebe, K. Structural Study on Cubic-Tetragonal Transition of CH3NH3PbI3. *J. Phys. Soc. Jpn.* **2002**, *71* (7), 1694−1697.

(16) Sendner, M.; Nayak, P. K.; Egger, D. A.; Beck, S.; Müller, C.; Epding, B.; Kowalsky, W.; Kronik, L.; Snaith, H. J.; Pucci, A.; Lovrinčic, R. Optical Phonons in Methylammonium Lead Halide Perovskites and Implications for Charge Transport. *Mater. Horiz.* **2016**, *3*, 1−8.

(17) Brivio, F.; Frost, J. M.; Skelton, J. M.; Jackson, A. J.; Weber, O. J.; Weller, M. T.; Goni, A. R.; Leguy, A. M. A.; Barnes, P. R. F.; Walsh, A. Lattice Dynamics and Vibrational Spectra of the Orthorhombic, Tetragonal, and Cubic Phases of Methylammonium Lead Iodide. *Phys. Rev. B: Condens. Matter Mater. Phys.* **2015**, *92* (14), 144308.

(18) Chang, Y. H.; Park, C. H.; Matsuishi, K. First-Principles Study of the Structural and the Electronic Properties of the Lead-Halide-Based Inorganic-Organic Perovskites (CH 3 NH 3)PbX 3 and CsPbX 3 (X = Cl, Br, I). *J. Korean Phys. Soc.* **2004**, *44* (4), 889−893.

(19) Motta, C.; El-Mellouhi, F.; Kais, S.; Tabet, N.; Alharbi, F.; Sanvito, S. Revealing the Role of Organic Cations in Hybrid Halide Perovskite CH3NH3PbI3. *Nat. Commun.* **2015**, *6*, 7026.

(20) Swainson, I. P.; Hammond, R. P.; Soullière, C.; Knop, O.; Massa, W. Phase Transitions in the Perovskite Methylammonium Lead Bromide, CH3ND3PbBr3. *J. Solid State Chem.* **2003**, *176* (1), 97−104.

(21) Swainson, I. P.; Stock, C.; Parker, S. F.; Van Eijck, L.; Russina, M.; Taylor, J. W. From Soft Harmonic Phonons to Fast Relaxational Dynamics in CH3NH3PbBr3. *Phys. Rev. B: Condens. Matter Mater. Phys.* **2015**, *92* (10), 2−6.

(22) Singh, S.; Li, C.; Panzer, F.; Narasimhan, K. L.; Graeser, A.; Gujar, T. P.; Köhler, A.; Thelakkat, M.; Huettner, S.; Kabra, D. Effect of Thermal and Structural Disorder on the Electronic Structure of Hybrid Perovskite Semiconductor CH3NH3PbI3. *J. Phys. Chem. Lett.* **2016**, *7*, 3014−3021.

(23) Elliott, R. J. Intensity of Optical Absorption by Excitons. *Phys. Rev.* **1957**, *108* (6), 1384−1389.

(24) Sestu, N.; Cadelano, M.; Sarritzu, V.; Chen, F.; Marongiu, D.; Piras, R.; Mainas, M.; Quochi, F.; Saba, M.; Mura, A.; Bongiovanni, G. Absorption F-Sum Rule for the Exciton Binding Energy in

Methylammonium Lead Halide Perovskites. *J. Phys. Chem. Lett.* **2015**, *6* (22), 4566−4572.
(25) Wright, A. D.; Verdi, C.; Milot, R. L.; Eperon, G. E.; Pérez-Osorio, M. A.; Snaith, H. J.; Giustino, F.; Johnston, M. B.; Herz, L. M. Electron−phonon Coupling in Hybrid Lead Halide Perovskites. *Nat. Commun.* **2016**, *7*, 11755.
(26) Kumar, A.; Kumawat, N. K.; Maheshwari, P.; Kabra, D. Role of Halide Anion on Exciton Binding Energy and Disorder in Hybrid Perovskite Semiconductors. *2015 IEEE 42nd Photovolt. Spec. Conf. PVSC 2015* **2015**, 8−11.
(27) Bokdam, M.; Sander, T.; Stroppa, A.; Picozzi, S.; Sarma, D. D.; Franchini, C.; Kresse, G. Role of Polar Phonons in the Photo Excited State of Metal Halide Perovskites. *Sci. Rep.* **2016**, *6*, 28618.
(28) Menéndez-Proupin, E.; Ríos, C. L. B.; Wahnón, P. Non-hydrogenic Exciton Spectrum in Perovskite CH3NH3PbI3. *Phys. Status Solidi RRL* **2015**, *9* (10), 559−563.
(29) Wehrenfennig, C.; Liu, M.; Snaith, H. J.; Johnston, M. B.; Herz, L. M. Homogeneous Emission Line Broadening in the Organo Lead Halide Perovskite CH3NH3PbI3- xClx. *J. Phys. Chem. Lett.* **2014**, *5* (8), 1300−1306.
(30) Cody, G. D.; Tiedje, T.; Abeles, B.; Brooks, B.; Goldstein, Y. Disorder and the Optical-Absorption Edge of Hydrogenated Amorphous Silicon. *Phys. Rev. Lett.* **1981**, *47* (20), 1480−1483.

DOI: 10.1021/acsami.6b15694
ACS Appl. Mater. Interfaces 2017, 9, 10344−10348